JCI The Journal of Clinical Investigation

Antihypertensive effects of selective prostaglandin E_2 receptor subtype 1 targeting

Youfei Guan, … , Richard M. Breyer, Matthew D. Breyer

J Clin Invest. 2007;117(9):2496-2505. https://doi.org/10.1172/JCI29838.

Research Article Cardiology

Clinical use of prostaglandin synthase–inhibiting NSAIDs is associated with the development of hypertension; however, the cardiovascular effects of antagonists for individual prostaglandin receptors remain uncharacterized. The present studies were aimed at elucidating the role of prostaglandin E_2 (PGE_2) E-prostanoid receptor subtype 1 (EP1) in regulating blood pressure. Oral administration of the EP1 receptor antagonist SC51322 reduced blood pressure in spontaneously hypertensive rats. To define whether this antihypertensive effect was caused by EP1 receptor inhibition, an EP1-null mouse was generated using a “hit-and-run” strategy that disrupted the gene encoding EP1 but spared expression of protein kinase N (PKN) encoded at the EP1 locus on the antiparallel DNA strand. Selective genetic disruption of the EP1 receptor blunted the acute pressor response to Ang II and reduced chronic Ang II–driven hypertension. SC51322 blunted the constricting effect of Ang II on in vitro–perfused preglomerular renal arterioles and mesenteric arteriolar rings. Similarly, the pressor response to EP1-selective agonists sulprostone and 17-phenyltrinor PGE_2 were blunted by SC51322 and in EP1-null mice. These data support the possibility of targeting the EP1 receptor for antihypertensive therapy.

Antihypertensive effects of selective prostaglandin E_2 receptor subtype 1 targeting

Youfei Guan,[1,2] Yahua Zhang,[1] Jing Wu,[2] Zhonghua Qi,[1] Guangrui Yang,[2] Dou Dou,[2] Yuansheng Gao,[2] Lihong Chen,[2] Xiaoyan Zhang,[2] Linda S. Davis,[1] Mingfeng Wei,[2] Xuefeng Fan,[1] Monica Carmosino,[1] Chuanming Hao,[1] John D. Imig,[3] Richard M. Breyer,[4] and Matthew D. Breyer[1,5]

[1]Division of Nephrology, Department of Medicine, Vanderbilt University Medical Center, Nashville, Tennessee, USA. [2]Department of Physiology and Pathophysiology, Peking University Health Science Center, Beijing, People's Republic of China. [3]Department of Physiology, Medical College of Georgia, Augusta, Georgia, USA. [4]Department of Pharmacology and [5]Department of Molecular Physiology and Biophysics, Vanderbilt University Medical Center, Nashville, Tennessee, USA.

Clinical use of prostaglandin synthase–inhibiting NSAIDs is associated with the development of hypertension; however, the cardiovascular effects of antagonists for individual prostaglandin receptors remain uncharacterized. The present studies were aimed at elucidating the role of prostaglandin E_2 (PGE_2) E-prostanoid receptor subtype 1 (EP1) in regulating blood pressure. Oral administration of the EP1 receptor antagonist SC51322 reduced blood pressure in spontaneously hypertensive rats. To define whether this antihypertensive effect was caused by EP1 receptor inhibition, an EP1-null mouse was generated using a "hit-and-run" strategy that disrupted the gene encoding EP1 but spared expression of protein kinase N (PKN) encoded at the EP1 locus on the antiparallel DNA strand. Selective genetic disruption of the EP1 receptor blunted the acute pressor response to Ang II and reduced chronic Ang II–driven hypertension. SC51322 blunted the constricting effect of Ang II on in vitro–perfused preglomerular renal arterioles and mesenteric arteriolar rings. Similarly, the pressor response to EP1-selective agonists sulprostone and 17-phenyltrinor PGE_2 were blunted by SC51322 and in EP1-null mice. These data support the possibility of targeting the EP1 receptor for antihypertensive therapy.

Introduction

Prostaglandins are endogenous oxygenated fatty acid metabolites and play important roles in inflammation as well as in modulating arterial blood pressure and renal salt excretion (1–3). The predominant effects of endogenous prostanoids are generally poised to reduce blood pressure, consistent with clinical observations that NSAIDs that inhibit prostaglandin synthase (cyclooxygenase; COX), such as COX2 inhibitors, cause hypertension (4–7). More recently, divergent cardiovascular effects of COX1 versus COX2 inhibition have been observed in mouse models of atherosclerosis and hypertension. Instead of exacerbating hypertension, chronic treatment with a selective COX1 inhibitor or COX1 gene knockout reduced the pressor effect of Ang II (8). Conversely, pretreatment with an oral COX2 inhibitor enhanced the pressor effect of Ang II. These findings support the possibility that COX2-derived prostaglandins reduce blood pressure, while COX1-derived prostaglandins increase blood pressure. The specific prostanoids that are responsible for these divergent effects of COX products on Ang II action remain poorly defined.

Endogenous prostaglandins include 5 major bioactive compounds: prostaglandin E_2 (PGE_2), prostaglandin $F_{2\alpha}$ ($PGF_{2\alpha}$), prostaglandin D_2 (PGD_2), prostacyclin (PGI_2), and thromboxane A_2 (TXA_2) (9). Each prostanoid exerts local biological effects via specific G protein–coupled receptors expressed on nearby target cells. PGE_2 is a major prostanoid synthesized in mouse kidney and vasculature (10). It is unique among the prostanoids in that it can activate 4 distinct G protein–coupled membrane receptors — designated E-prostanoid receptor 1 (EP1), EP2, EP3, and EP4 — that are encoded by different genes and exhibit different tissue distribution (1, 9). These EP receptors can be selectively activated by different structural PGE_2 analogs, and each receptor activates different cell signaling pathways (11, 12). Infusion of PGE_2 i.v. in mice causes a transient fall in blood pressure, while disruption of the EP2 receptor unmasks a pressor response to PGE_2 (13), consistent with a depressor role for the EP2 receptor. In the absence of EP2, the pressor effects of PGE_2 are presumably mediated by the remaining receptors, possibly EP1 or EP3. Because Ang II stimulates PGE_2 synthesis (10, 14, 15), endogenous PGE_2 could modulate Ang II action in either a pressor or a depressor fashion.

The contribution of endogenous EP receptors to hypertension remains incompletely characterized. Both EP1 receptor antagonists (16–18) and EP1 knockout mice exist, but have not been characterized in models of hypertension. While conventional targeting of the gene encoding EP1 in mice suggests a role for EP1 in maintaining basal blood pressure (19), interpretation of these data is complicated by the circumstance that the EP1 locus encompasses a second gene on the antiparallel strand, the serine/threonine protein kinase N (PKN) (20). PKN is homologous to PKC and activated by rho GTPase and by fatty acids including arachidonate, and so might contribute to the regulation of vascular tone independent of EP1 (21). The aim of the present studies was to elucidate the role of the EP1 receptor in hypertension using an EP1 receptor–specific antagonist and an EP1 knockout mouse (*Ptger1*$^{-/-}$, referred to herein as EP1$^{-/-}$) that disrupts EP1 while sparing the PKN locus. Our findings demonstrate that either an EP1 receptor antagonist or EP1 receptor disruption ameliorate hypertension, supporting the feasibility of targeting the EP1 receptor for antihypertensive therapy.

Nonstandard abbreviations used: $[Ca^{2+}]_i$, intracellular calcium; COX, cyclooxygenase; EP, E-prostanoid receptor; MAP, mean arterial blood pressure; PGE_2, prostaglandin E_2; PKN, protein kinase N; SHR, spontaneously hypertensive rat; TK, thymidylate kinase; 3′ UTR, 3′ untranslated region.

Conflict of interest: The authors have declared that no conflict of interest exists.

Citation for this article: *J. Clin. Invest.* **117**:2496–2505 (2007). doi:10.1172/JCI29838.

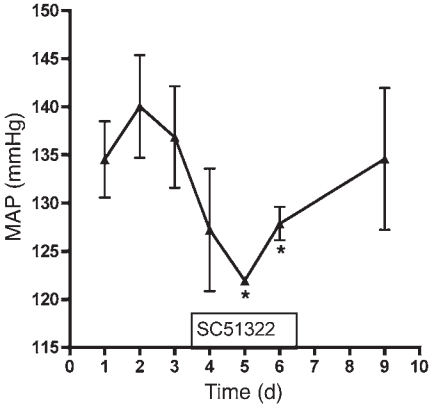

Figure 1
Effect of the EP1 receptor antagonist SC51322 (10 mg/kg/d by gavage) on MAP as determined by radiotelemetry in SHRs. Values are mean ± SEM (n = 3). *P < 0.05 versus baseline, paired 2-tailed Student's t test.

Results

Pharmacologic blockade of the EP1 receptor reduces blood pressure in the spontaneously hypertensive rat. The spontaneously hypertensive rat (SHR) is a well established model of hypertension (22). SC51322 is a selective and potent EP1 receptor antagonist, and was originally developed as an analgesic (17, 23, 24). The effect of SC51322 on blood pressure in SHRs was assessed using daily radiotelemetric recordings of mean arterial blood pressure (MAP). Treatment with SC51322 (10 mg/kg/d orally) significantly reduced MAP over 3 days of treatment without affecting heart rate. Following discontinuation of SC51322 treatment, MAP returned to elevated levels (Figure 1). These results suggest that EP1 receptor activation contributes to hypertension in the SHR model.

Generation of EP1$^{-/-}$ mice. To confirm a role for the EP1 receptor in promoting hypertension, we generated what we believe to be a novel EP1 knockout mouse. Because the EP1 locus overlaps the PKN locus on the antiparallel strand (20), we selectively targeted the EP1 locus using a "hit-and-run" targeting strategy (25), wherein a premature stop codon (R242X) linked in tandem with a newly created EcoRI restriction site (Figure 2C) was introduced into exon 2 (Figure 2 and Supplemental Figure 1; supplemental material available online with this article; doi:10.1172/JCI29838DS1). Following neomycin selection of ES cells targeted at the EP1 locus, the ES cells were selected for thymidylate kinase–resistant (TK-resistant) revertants in which the neomycin and TK cassettes were excised by an internal crossover event, leaving behind the 3-bp change in EP1 coding sequence and in the 3′ untranslated region (3′ UTR) of the long PKN transcript (Supplemental Figure 1). Wild-type and targeted EP1 alleles were genotyped using both Southern blot and PCR-based methods (Supplemental Figure 1).

The presence of the expected premature in-frame stop codon and EcoRI site in the mutant EP1 mRNA was demonstrated using RT-PCR to amplify a 780-bp fragment spanning the mutant nucleotides from cDNAs obtained from EP1$^{+/+}$ or EP1$^{-/-}$ mouse kidney (Figure 2C). The PCR product amplified from EP1$^{+/+}$ mouse kidney cDNA was resistant to the EcoRI digestion, while PCR fragments from the EP1$^{-/-}$ mouse kidney cDNAs were cleaved into fragments of 670 bp and 110 bp. This demonstrated the presence of the EcoRI in mutant EP1 mRNA (Figure 2D), as was additionally confirmed by sequencing the PCR fragments (data not shown).

Disrupted signaling by EP1 receptor mutant. We confirmed that PGE_2 failed to elicit the expected signaling events in HEK293 cells stably transfected with the mutant EP1 expression vector. The EP1 receptor signals via increased intracellular Ca^{2+} ($[Ca^{2+}]_i$) (26–28), as seen in fura-2–loaded HEK293 cells transfected with EP1$^{+/+}$ vector and treated with PGE_2 (Figure 2E). In contrast, in untransfected HEK293 cells or cells expressing the mutant EP1 receptor, PGE_2 failed to increase $[Ca^{2+}]_i$ (P < 0.005).

PKN expression is unaffected in EP1-targeted mice. In situ hybridization detected renal expression of both PKN and EP1 in a nonoverlapping distribution, with PKN expression predominating in the renal cortex and EP1 predominating in the renal medulla (Figure 2F). Identical intrarenal localization of PKN was seen in EP1$^{+/+}$ and EP1$^{-/-}$ mice (Figure 2G). PKN expression was also studied in immunoprecipitates from kidneys and whole brains of EP1$^{+/+}$ and EP1$^{-/-}$ mice, and PKN protein levels were comparable between groups. These results confirm that the 3-bp change in the 3′ UTR of the long transcript did not affect PKN expression.

Role of the EP1 receptor in the pressor response to Ang II. Having confirmed that the truncation mutation disrupted EP1 receptor function, we examined whether EP1 receptor disruption affects the acute pressor response to i.v. Ang II infusion (75 pmol/kg/min) by using indwelling carotid catheter in anesthetized male 129S6/SvEvTac mice. MAP was significantly reduced in EP1$^{-/-}$ versus EP1$^{+/+}$ mice (Figure 3A), with a peak increase in MAP of 20.9 ± 4.7 mmHg in EP1$^{-/-}$ mice after Ang II versus 26.2 ± 2.7 mmHg in EP1$^{+/+}$ mice (P < 0.005). This reduction in the hypertensive response to Ang II was sustained for the duration of its infusion (P < 0.01; Figure 3B).

To further explore the role of EP1 receptor deletion on blood pressure regulation, a model of Ang II–dependent hypertension was established in wild-type male N10 129S6/SvEvTac EP1$^{+/+}$ and EP1$^{-/-}$ littermates using chronic Ang II infusion (1,000 ng/kg/min s.c.; n = 5 per genotype). Systolic arterial blood pressure, measured both by tail-cuff method in conscious mice and by preterminal carotid catheterization in the same mice following anesthesia (13, 29), was significantly greater in EP1$^{+/+}$ mice than in EP1$^{-/-}$ mice (P < 0.0001; Figure 3C). Baseline tail-cuff systolic blood pressure in male 129S6/SvEvTac mice was slightly, but significantly, lower in EP1$^{-/-}$ than in EP1$^{+/+}$ mice (113.20 ± 2.97 versus 119.84 ± 2.18 mmHg; n = 5; P < 0.001; Figure 3C). While Ang II significantly increased systolic blood pressure in both genotypes (Figure 3C), the increase in systolic blood pressure was significantly greater in EP1$^{+/+}$ mice than EP1$^{-/-}$ mice (26 ± 1.1 versus 18 ± 1.1 mmHg; P < 0.0001; Figure 3D). Over the 4-week period of Ang II infusion, systolic blood pressure averaged approximately 16 mmHg lower in EP1$^{-/-}$ mice compared with EP1$^{+/+}$ mice (P < 0.001), and this significant difference in MAP was confirmed at the end of the 4-week Ang II period by direct intracarotid measurements (Figure 3E). Furthermore, Ang II–associated cardiac hypertrophy was significantly reduced in EP1$^{-/-}$ mice compared with EP1$^{+/+}$ mice (164 ± 5 versus 186 ± 21 mg; n = 5 and 4, respectively; P = 0.045). This difference in cardiac weight was maintained when corrected for body weight (6.0 ± 0.18 versus 7.1 ± 0.48 mg heart wt/g body wt; P = 0.05).

Arteriolar response to angiotensin following EP1 blockade. The effect of EP1 receptor blockade on the renal afferent arteriolar response to angiotensin was determined. Afferent arteriolar diameter averaged 17.4 ± 0.6 μm (n = 14). Angiotensin dose-dependently decreased afferent arteriolar diameter, and this vascular response was significantly attenuated in the presence of the EP1 receptor antagonist

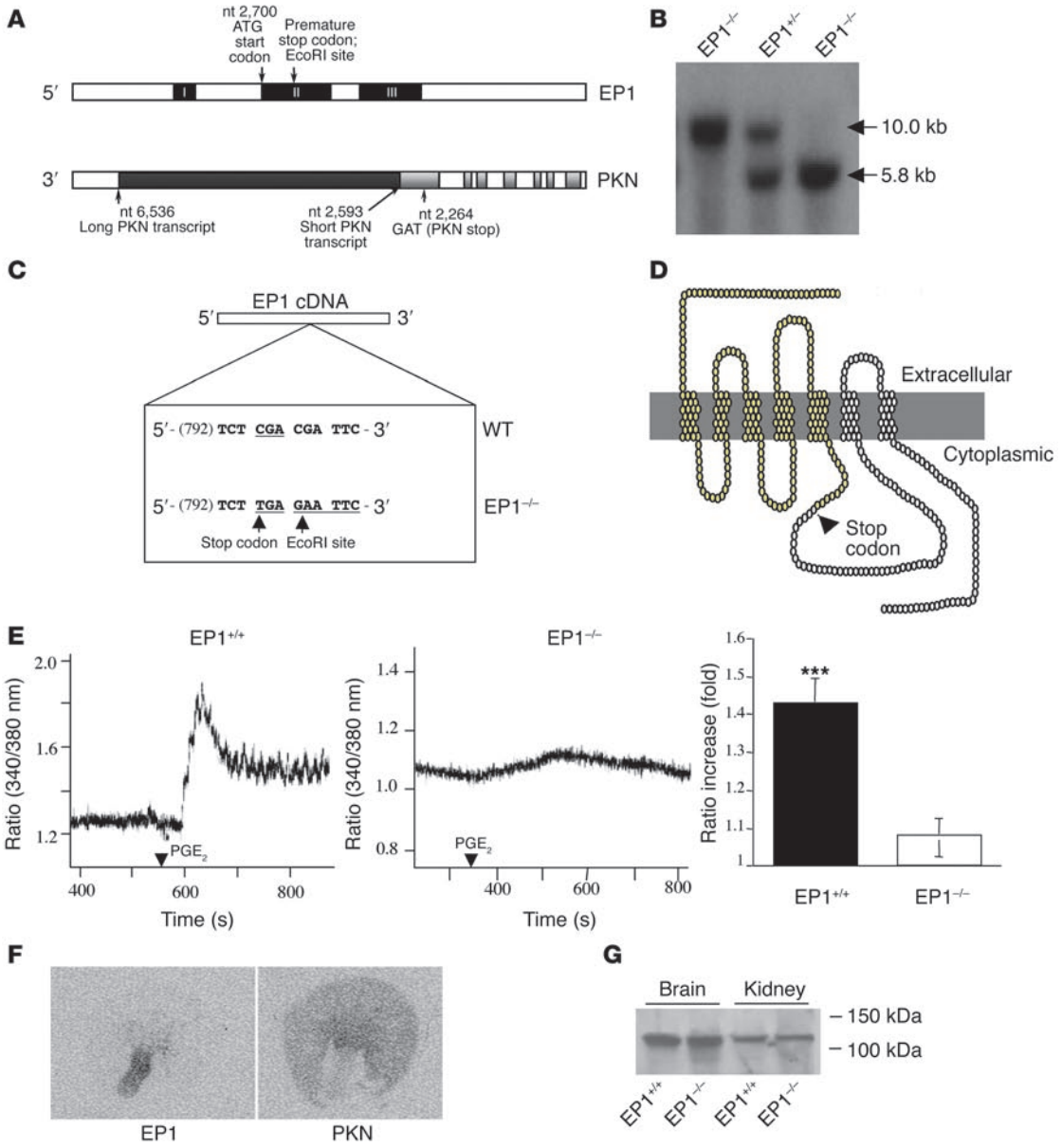

Figure 2

Generation and characterization of a hit-and-run–targeted EP1$^{-/-}$ mouse. (**A**) Genomic organization of mouse EP1 and PKN genes. The EP1 gene consists of 3 exons (black boxes) spanning approximately 7.2 kb. Shown are the translational ATG start site (nucleotides 2,700–2,702) and the premature stop codon and EcoRI site introduced in the mutant. PKN is antiparallel with EP1, and 2 alternative 3′ splice variants (arrows) are characterized by differences in the 3′ UTR. (**B**) Southern blot of EcoRI digest demonstrated successful incorporation of the EcoRI site into the EP1$^{-/-}$ mouse. The radiolabeled EP1 probe recognized a 10-kb EcoRI fragment derived from the wild-type allele and a 5.8-kb fragment from the mutant allele. (**C**) Design of EP1$^{+/+}$ and EP1$^{-/-}$ cDNA. The C795T mutation in knockout cDNA caused an in-frame R242X stop codon (CGA to TGA). Additionally, mutations C798G and G799A created a new EcoRI restriction site. (**D**) Secondary structure of EP1 receptor showing the site of truncation in the mutant receptor following the putative fifth membrane–spanning α-helix. (**E**) $[Ca^{2+}]_i$ signaling in fura-2–loaded HEK293 cells transfected with EP1$^{+/+}$ and EP1$^{-/-}$ cDNA was determined using the 340/380 nm emission intensity ratio. PGE_2 (1 μM) significantly increased the ratio above basal values in cells transfected with EP1$^{+/+}$ expression vector but not in HEK293 cells transfected with EP1$^{-/-}$. (**F**) Autoradiogram in situ hybridization showed distribution of ^{35}S-labled riboprobes for EP1 antisense and PKN (EP1 sense) probes demonstrating nonoverlapping and inverse distribution patterns in mouse kidney. (**G**) Immunoprecipitation of EP1$^{+/+}$ and EP$^{-/-}$ mouse kidney and brain lysates showed PKN expression was not altered in EP1$^{-/-}$ mice.

SC51322 (1 μM; Figure 3H). The vascular response to the EP1 and EP3 receptor agonist 17-phenyltrinor PGE_2 was also determined. Afferent arteriolar diameter decreased by 19% ± 4% (n = 7) in response to 1 μM 17-phenyltrinor PGE_2.

Mesenteric arteriolar tension. Expression of EP1 receptor was demonstrated by RT-PCR using mRNA obtained from mesenteric arteries, a systemic resistance vessel. The specificity of the PCR product was confirmed by sequencing and absence of a PCR product

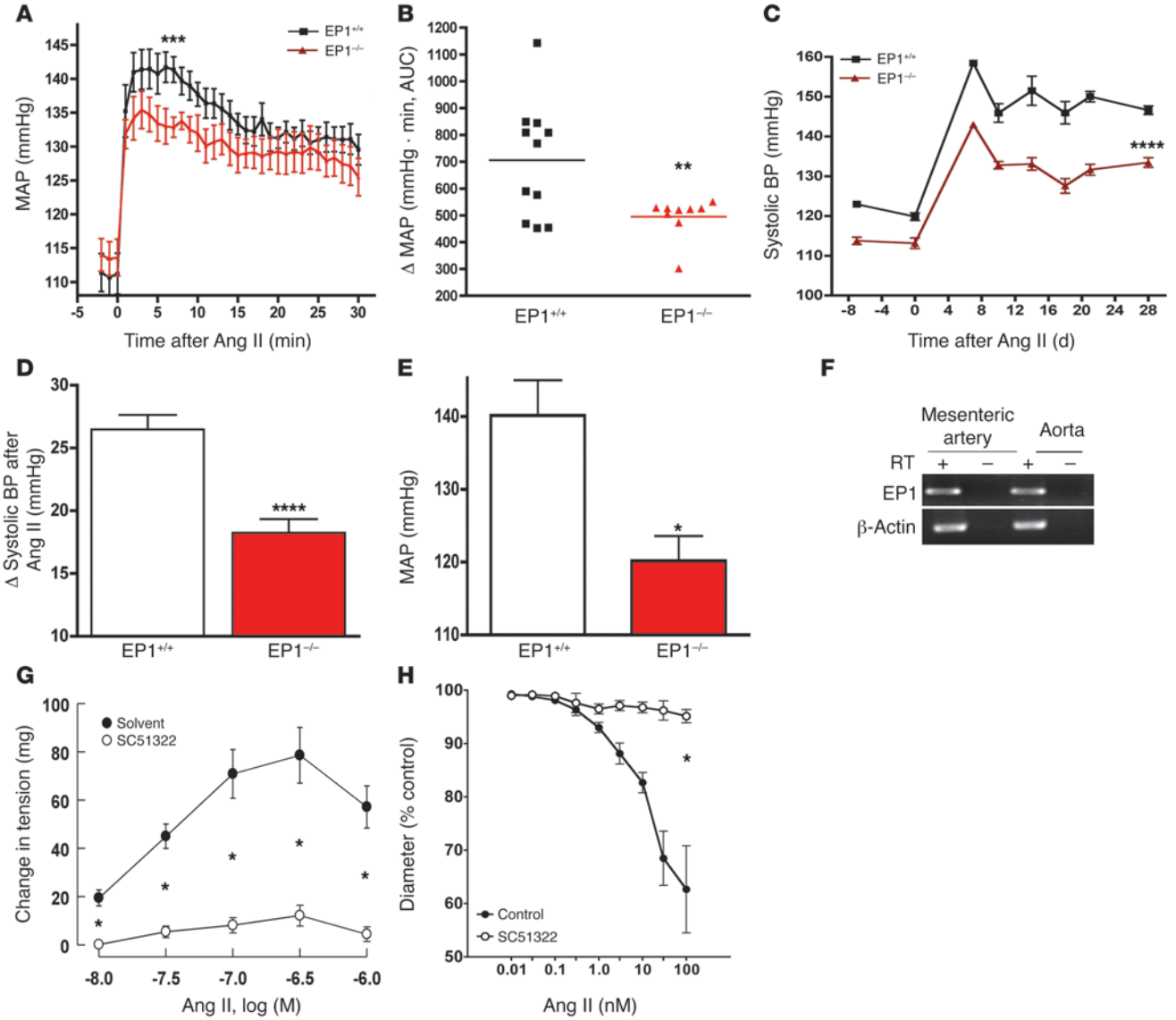

Figure 3

Effect of EP1 gene disruption on in vivo effects of Ang II. (**A**) Reduced pressor response to Ang II in EP1$^{-/-}$ versus EP1$^{+/+}$ mice. MAP was recorded by intracarotid arterial monitoring before and during i.v. infusion of Ang II (75 pmol/kg/min). $n = 8$ per group. ***$P < 0.005$. (**B**) The pressor response to Ang II integrated over time was significantly reduced in EP1$^{-/-}$ compared with EP1$^{+/+}$ mice. AUC, area under the curve. **$P < 0.01$. (**C**) Effect of chronic Ang II infusion (1,000 ng/kg/min) on systolic blood pressure determined by tail cuff. Baseline blood pressure was significantly lower in EP1$^{-/-}$ mice than in EP1$^{+/+}$ mice ($n = 5$ per group) and the difference between genotypes increased following Ang II infusion. ***$P < 0.001$; ****$P < 0.0001$. (**D**) The change in systolic blood pressure following Ang II minipump was significantly greater in EP1$^{+/+}$ than in EP1$^{-/-}$ mice ($n = 5$). ****$P < 0.0001$. (**E**) MAP determined by intracarotid catheterization was significantly greater in EP1$^{+/+}$ ($n = 3$) than in EP1$^{-/-}$ ($n = 4$) mice infused with Ang II. *$P < 0.05$. (**F**) Expression of EP1 receptor mRNA in microdissected mouse mesenteric arteries and aortic tissue. Lack of RT was utilized as a negative control and β-actin served as RNA loading control. (**G**) Reduced constriction of Ang II on in vitro mesenteric arteriolar rings following pretreatment with the EP1 receptor antagonist SC51322. $n = 7$ per group. (**H**) Reduced Ang II constriction of preglomerular arterioles following treatment with EP1 receptor antagonist SC51322 (1 μM). $n = 7$ per group. *$P < 0.005$.

using mRNA as template without reverse transcription. Both dissected mouse mesenteric arteries and aortas were found to express EP1 receptor mRNA (Figure 3F). These findings support a model whereby the EP1 receptor directly exerts its systemic pressor activity on arterial resistance vessels.

Ang II induced concentration-dependent contraction of isolated mouse mesenteric arterioles. The maximal contraction was obtained using 10^{-7} M Ang II. While the EP1 receptor blocker SC51322 (10^{-6} M; ref. 17) had no effect on the basal tension ($n = 7$; $P > 0.05$; data not shown), it almost completely eliminated Ang II–evoked contraction (Figure 3G).

Effect of EP1 receptor agonists on MAP. To examine whether EP1 receptor disruption alters regulation of blood pressure by infusion of PGE_2, PGE_2- and EP-specific analogs were performed. The pressor effect of the EP1/EP3 receptor–selective agonist 17-phenyltrinor PGE_2 was markedly reduced in male EP1$^{-/-}$ mice, increasing MAP by

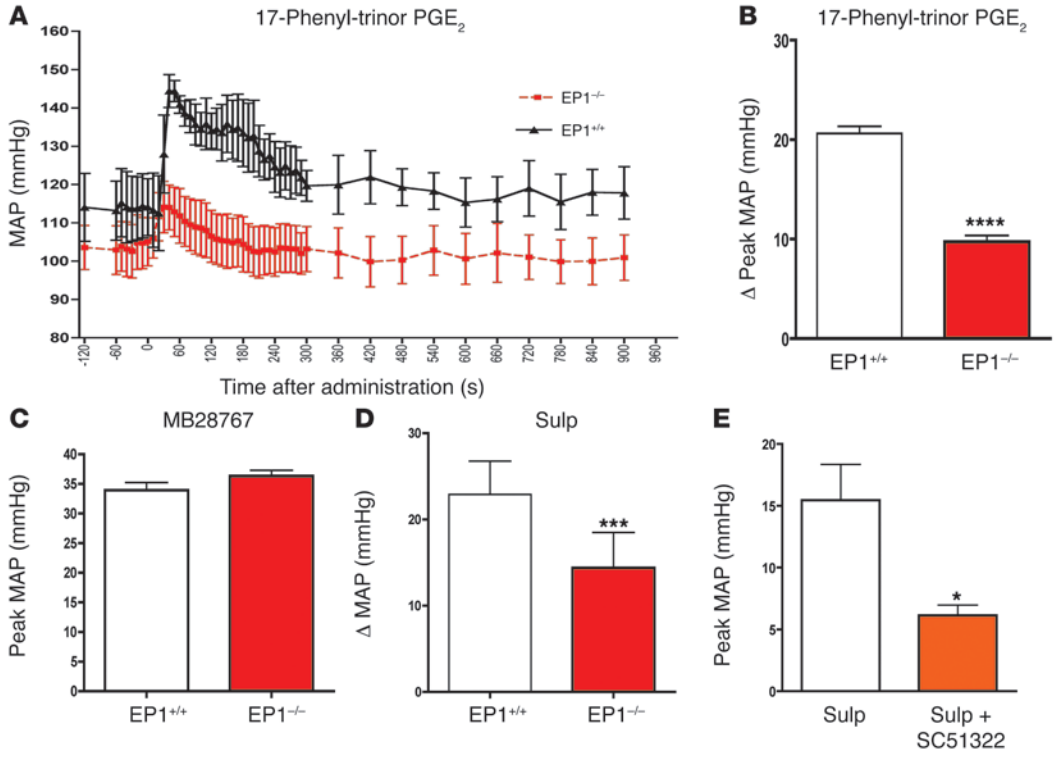

Figure 4

Effect of i.v. infusion of EP1/EP3 receptor agonists on MAP in EP1$^{-/-}$ and EP1$^{+/+}$ mice. (**A**) Temporal course showing reduced pressor effects of the mixed EP1/EP3 agonist 17-phenyltrinor PGE_2 (20 μg/kg i.v. bolus) in EP1$^{-/-}$ (n = 5) versus EP1$^{+/+}$ (n = 3) mice. $P < 0.0001$, repeated-measures 2-way ANOVA. (**B**) Increase in peak MAP (at about 40–70 s) following 17-phenyltrinor PGE_2 (20 μg/kg i.v. bolus) was significantly less in EP1$^{-/-}$ than in EP1$^{+/+}$ mice. ****$P < 0.0001$. (**C**) Identical peak pressor response to the pure EP3 agonist MB28767 in EP1$^{-/-}$ (n = 3) and EP1$^{+/+}$ (n = 4) mice. (**D**) The peak pressor response to sulprostone (Sulp), another EP1/EP3 agonist, was reduced in EP1$^{-/-}$ mice. ***$P < 0.001$. (**E**) Pretreatment of mice with the EP1-selective agonist SC51322 (n = 5) significantly reduced the peak pressor response to sulprostone. *$P < 0.05$.

9.7 ± 0.6 versus 20.6 ± 0.7 mmHg in EP1$^{+/+}$ littermates ($P < 0.0001$; Figure 4, A and B). The blunted vasopressor effect of 17-phenyltrinor PGE_2 is consistent with a systemic vasopressor role for the EP1 receptor. Because 17-phenyltrinor PGE_2 also has activity at the EP3 receptor, we also tested the effect of a pure EP3 agonist, MB28767, on blood pressure in EP1$^{+/+}$ and EP1$^{-/-}$ mice. MB28767 produced a maximal pressor effect in EP1$^{-/-}$ mice identical to that observed in EP1$^{+/+}$ littermates (Figure 4C), suggesting the diminished pressor activity of the 17-phenyltrinor PGE_2 was due to lack of a pressor EP1 receptor activity, rather than an effect on EP3 receptor.

Sulprostone, another EP1/EP3 agonist, also exhibited blunted pressor activity in EP1$^{-/-}$ mice (Figure 4D). Similarly, pretreatment of EP1$^{+/+}$ mice with selective EP1 receptor antagonist SC51322 significantly blunted the pressor effect of sulprostone (Figure 4E). In contrast, administration of EP1 receptor antagonist SC51322 had no effect on the pressor activity of sulprostone in EP1$^{-/-}$ mice (data not shown). The residual pressor effect of sulprostone in EP1$^{-/-}$ mice may be attributable to a separate pressor action of this agonist via the EP3 receptor.

Previous studies using a standard EP1 knockout generated in DBA1 mice suggested that deletion of the EP1 receptor reduced the vasodepressor response to the endogenous EP ligand, PGE_2 (30). The present studies also found a modest reduction in the vasodepressor response to PGE_2 (100 μg/kg i.v.) in male 129S6/SvEv EP1$^{-/-}$ mice (n = 8 per group; $P < 0.005$; Figure 5, A and B). To further characterize the mechanism underlying this difference, we tested the vascular effects of i.v. infusion of the vasodepressor EP2 and EP4 agonists (31) in EP1$^{-/-}$ mice. Although the vasodepressor effect of the EP2 agonist butaprost was similar in EP1$^{+/+}$ and EP1$^{-/-}$ mice (Figure 5C), the vasodepressor effect of the preferential EP4 agonist PGE_1-OH was significantly blunted in EP1$^{-/-}$ mice (Figure 5D), consistent with a functional interaction between vascular EP1 and EP4 receptors.

Effect of the EP1 receptor on renal salt and urine excretion. Acute infusion of PGE_2 did not affect urine volume or sodium excretion in either EP1$^{-/-}$ or EP1$^{+/+}$ mice (data not shown). Furthermore, no differences in plasma aldosterone in EP1$^{+/+}$ versus EP1$^{-/-}$ mice on standard (0.25% w/w) NaCl diet were observed (835 ± 105 versus 695.9 ± 45 pg/ml; P = NS). To further examine whether the EP1 receptor affects renal salt or water excretion, we measured urine volume and sodium and potassium excretion in EP1$^{+/+}$ and EP1$^{-/-}$ mice sequentially placed on diets containing 0.25%, 0.02%, and 8% (w/w) NaCl. Urine volume and sodium excretion were significantly greater in EP1$^{+/+}$ than in EP1$^{-/-}$ mice following the switch from low- to high-sodium diet; however, this was accompanied by greater water and food intake in EP1$^{+/+}$ mice (Figure 6). Despite these differences in dietary sodium and water intake and excretion, systolic blood pressure remained unchanged in EP1$^{-/-}$ mice and significantly lower than in EP1$^{+/+}$ mice (Figure 6).

Discussion

The present studies demonstrate that endogenous EP1 receptor activation contributes to hypertension in 2 well-established rodent models: the SHR and chronic Ang II infusion. This conclusion is independently supported by results using what we believe to be a novel EP1$^{-/-}$ mouse and an EP1-selective receptor antagonist SC51322 (32). The latter not only reduced blood pressure in SHRs but also blocked the acute pressor effect of the EP1/EP3 agonist sulprostone in mice. Whether prolonged treatment with SC51322 results in a persistent reduction in blood pressure remains to be determined; however, a role for EP1 receptor antagonism is further

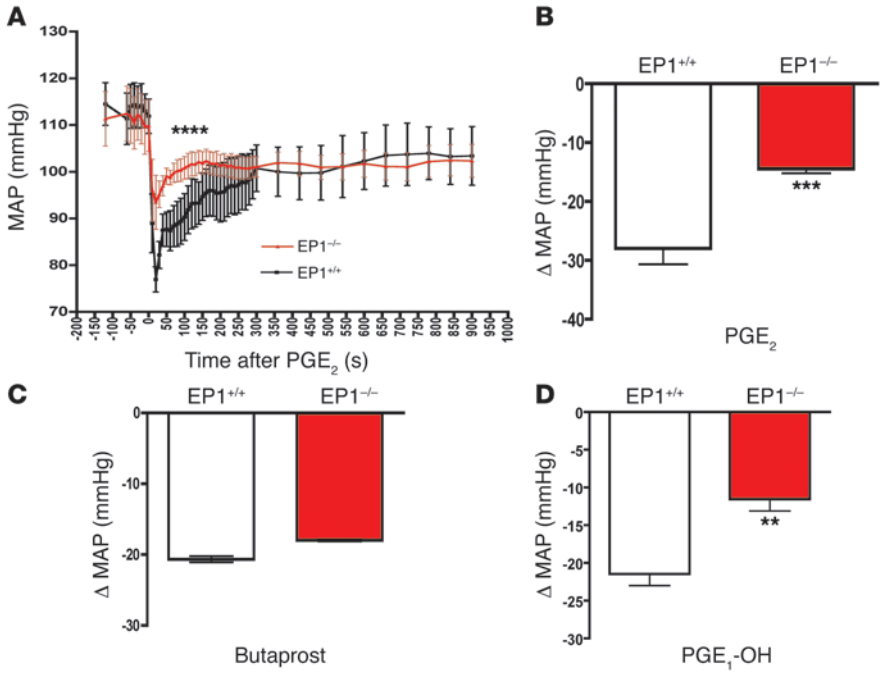

Figure 5
Effects of vasodepressor PGE_2 analogs. (**A**) Time course showing reduced vasodepressor response to PGE_2 (100 μg/kg) in $EP1^{-/-}$ versus $EP1^{+/+}$ mice. $n = 8$ per group. $^{****}P < 0.0001$, repeated-measures 2-way ANOVA. (**B**) $EP1^{-/-}$ mice exhibited a reduced vasodepressor response nadir following bolus PGE_2 infusion. $^{***}P < 0.005$. (**C**) No difference was observed in MAP reduction following i.v. infusion of the EP2-selective agonist butaprost (20 μg/kg) in $EP1^{-/-}$ ($n = 4$) versus $EP1^{+/+}$ ($n = 3$) mice. (**D**) $EP1^{-/-}$ mice exhibited a reduced vasodepressor response nadir in MAP following bolus infusion of the EP4-selective agonist PGE_1-OH (100 μg/kg i.v.). $^{**}P < 0.01$.

supported by findings that genetic disruption of the EP1 receptor in mice was associated with both sustained reduction in blood pressure and reduced cardiac weight following 4 weeks of Ang II infusion. Our results add to previous reports that endogenous COX products contribute to the vasoconstrictor activity of Ang II (10, 33) and are consistent with the prior finding that altered PGE_2 action is involved in the pathogenesis of hypertension in SHRs (34). Notably, in contrast to the effects of prostaglandin synthase inhibition by NSAIDs, selective EP1 receptor inhibition reduced blood pressure, rather than increasing it.

The mechanism by which EP1 receptor disruption ameliorates hypertension is consistent with an altered vascular response to Ang II, as supported by the observation that $EP1^{-/-}$ mice exhibited a reduced acute vasopressor effect of Ang II infusion. This is further supported by the reduced pressor effect caused by the EP1 agonists sulprostone and 17-phenyltrinor PGE_2 in $EP1^{-/-}$ mice, or following pretreatment with the EP1 antagonist SC51322. Expression of EP1 receptor mRNA was demonstrated in peripheral resistance vessels and aortas, demonstrating vascular expression of the EP1 receptor. Direct functional interaction between angiotensin and EP1 receptor activity was demonstrated in in vitro mesenteric arterioles and preglomerular resistance arterioles, in which constrictor effects of Ang II were dramatically attenuated by the EP1 receptor antagonism, consistent with dependence of Ang II vasoconstriction on the EP1 receptor.

Gene targeting has proven a valuable tool for examining the biological roles of prostaglandin receptors (35). However, interpretation of the cardiovascular phenotypes in $EP1^{-/-}$ animals is complicated by the fact that the EP1 locus encodes both the EP1 receptor and PKN on the antiparallel strand (20). PKN is a serine/threonine protein kinase involved in PKC regulation and *Rho* function (21). Conventional gene targeting strategy uses the placement of an approximately 2-kb neomycin resistance cassette within the EP1 locus, and in this case could alter both the EP1 receptor and PKN transcripts. Although previous studies did not describe differences in PKN expression, immunoblots presented in those studies do not exclude the possibility of reduced PKN protein expression in $EP1^{-/-}$ mice (19). To circumvent alterations in PKN expression, we used a hit-and-run strategy whereby a premature stop codon was introduced in exon 2 of the EP1 locus and only 3 nucleotides were changed in the 3′ UTR of the PKN gene. As expected, altered PKN protein expression was not observed in $EP1^{-/-}$ mice generated in the present studies.

Despite concerns regarding PKN effects, many of the present findings are consistent with previous studies of standard DBA/1*lac*J $EP1^{-/-}$ mice (19). Both $EP1^{-/-}$ strains exhibited reduced basal blood pressure compared with $EP1^{+/+}$ mice. In addition to its presence in arterial vasculature, the EP1 receptor is abundantly expressed in the renal collecting duct (36). The authors of the previous study speculated that the lower baseline blood pressure in $EP1^{-/-}$ mice was the result of renal sodium wasting, but did not perform studies directly testing this hypothesis (19). From our analysis of urinary sodium and water excretion, we failed to find any evidence for sodium wasting: during sodium restriction, there was no difference in sodium retention or in serum aldosterone levels between $EP1^{-/-}$ and $EP1^{+/+}$ mice. Nor did we observe an acute drop in blood pressure over 3 days of salt restriction.

High salt intake also failed to normalize systolic blood pressure in $EP1^{-/-}$ mice. Previous studies of mice with collecting duct–specific modulation of endothelin-1 show the increase in blood pressure occurs within 1–2 days of instituting a high sodium diet (37), so the time frame of the present studies should have been adequate to discriminate a hypotensive phenotype due to EP1 action in the collecting duct. In contrast, on a high-salt diet, $EP1^{-/-}$ mice exhibited reduced rather than enhanced natriuresis and diuresis compared with $EP1^{+/+}$ mice. While this is consistent with a role for the EP1 receptor in modulating either renal salt and water excretion (or dietary sodium and water intake), reduced sodium excretion on a high-salt diet is not consistent with sodium wasting being the primary cause of lower blood pressure in $EP1^{-/-}$ mice. Conversely, reduced sodium excretion on a high-salt

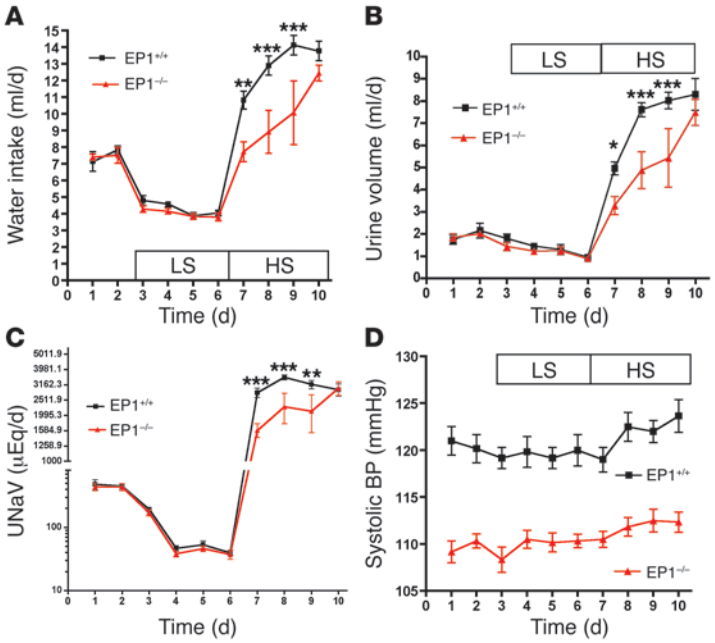

Figure 6

Effect of dietary sodium on water intake, urine volume, sodium excretion, and systolic blood pressure in 129S6/SvEvTac EP1$^{-/-}$ and EP1$^{+/+}$ mice. (**A**) Water intake in EP1$^{-/-}$ and EP1$^{+/+}$ mice ingesting normal 0.25% (w/w) NaCl diet, followed by low-salt 0.02% NaCl diet (LS) and high-salt 8% NaCl diet (HS). $^{**}P < 0.01$; $^{***}P < 0.001$. (**B**) Urine in EP1$^{-/-}$ and EP1$^{+/+}$ mice on normal-, low-, and high-salt diet. $^{*}P < 0.05$. $^{***}P < 0.001$, ANOVA. (**C**) Sodium excretion over a 24-hour period in EP1$^{-/-}$ and EP1$^{+/+}$ mice. $^{**}P < 0.01$; $^{***}P < 0.001$. UNaV, urine Na concentration multiplied by urine volume. (**D**) Systolic blood pressure was lower in EP1$^{-/-}$ mice than in EP1$^{+/+}$ mice and was not affected by dietary sodium intake.

diet is consistent with in vitro–microperfused collecting duct studies showing that EP1 receptor activation inhibits renal sodium absorption and could facilitate natriuresis (38). Collecting duct–mediated natriuresis may be particularly evident on high-sodium diets, which increase renal medullary COX2 expression and local PGE_2 synthesis (39). The EP1 receptor has also been identified in the hypothalamus where it could modulate dietary salt preference and thirst (40).

Pharmacologic studies using EP-selective agonists and antagonists demonstrate that EP1 receptors increase cytosolic calcium concentration via the G_q signaling pathway. The truncation mutation engineered into the EP1$^{-/-}$ mouse disrupted calcium signaling and was also associated with a dramatic reduction in the pressor effects of EP1 agonists including 17-phenyltrinor, PGE_2, and sulprostone. In contrast, EP2 and EP4 receptors, which preferentially link to G_s, stimulate cAMP generation (11, 12) and contribute to the vasodepressor effect of i.v. PGE_2 infusion (31). Unexpectedly, the maximal drop of blood pressure induced by the endogenous pan-EP receptor agonist PGE_2 was somewhat less in EP1$^{-/-}$ than in EP1$^{+/+}$ mice. A similar observation was made in a standard EP1$^{-/-}$ allele and was ascribed to direct vasodepressor activity of the EP1 receptor (30). The present findings using EP-selective agonists suggest a more complex mechanism, because the EP4-selective agonist PGE_1-OH, which has an exceedingly low affinity for the EP1 receptor (41, 42), also exhibited reduced vasodepressor activity in EP1$^{-/-}$ mice. In contrast, the EP2-selective agonist butaprost reduced blood pressure to a similar absolute value in EP1$^{-/-}$ mice and EP1$^{+/+}$ mice. These findings are consistent with a functional interaction between the EP1 and EP4 receptors. Although the precise mechanism(s) involved in this unexpected phenomenon remain speculative, one possibility is that EP1 receptor activity in endothelium contributes to EP4 receptor–dependent generation of vasodilators (e.g., nitric oxide), because both of these receptors have been identified in endothelial cells (43) and heterodimerization and crosstalk between prostanoid receptors has been suggested (44, 45).

PGE_2 is a major COX product of vascular smooth muscle, and Ang II stimulates its synthesis in this tissue (46–48). Recent studies implicate COX1 activity in promoting PGE_2 synthesis (10) and as critical for the pressor response to Ang II in both acute and chronic Ang II–dependent models (33, 49). The present data are consistent with a model whereby Ang II–stimulated synthesis of COX1-derived PGE_2 activates the EP1 receptor to promote Ang II–dependent hypertension. The vasodepressor effect of the EP1 antagonist in the SHR is also consistent with the possibility that the EP1 receptor may act as a tonic vasoconstrictor contributing to hypertension. Recent studies of Ang II–induced hypertension used kidney crosstransplantation in AT1a knockout mice to and from wild-type mice to define nonredundant pressor roles for intrarenal and extrarenal AT1a receptors through which Ang II increases blood pressure (50). The present findings support hemodynamic effects of EP1 receptors promoting Ang II–dependent hypertension. Thus, as opposed to classic NSAID action, which enhances vasomotor tone and increases blood pressure (6, 51), EP1 receptor antagonism reduces blood pressure. The EP1 receptor may provide a novel target for the treatment of hypertension.

Methods

Chemical and molecular reagents. PGE_2 and PGE_1-OH were purchased from Cayman Chemical and BioMol Research Laboratories. Sulprostone was provided by Berlex Laboratories. MB28767 was generously provided by M. Caton (Rhone-Poulenc Rorer, Dagenham, United Kingdom). Butaprost and 17-phenyltrinor PGE_2 were purchased from Cayman Chemical. SC51322 was purchased from BioMol Research Laboratories.

Construction of EP1 targeting vector and generation of EP1$^{-/-}$ mice using the hit-and-run strategy. All studies performed on rodents were reviewed and approved by the Institutional Animal Care and Use Committees of the Medical College of Georgia and Vanderbilt University. Mouse genomic clones containing the EP1 locus were obtained by screening a 129SVJ/ola genomic P1 library (Genome Systems) with a 233-bp murine EP1 cDNA fragment from the coding region of exon 2. A positive P1 clone was mapped by restriction enzyme digestion, and an EcoRI I fragment of 12 kb was sequenced. A 5,067-bp fragment containing all 3 exons of the EP1 gene was subcloned into pBluescript (Stratagene) by digesting with HindIII and XbaI. An 895-bp fragment was then amplified from this clone, and its sequence was altered using PCR-based mutagenesis. The mutations introduce a stop codon in the coding region of the EP1 receptor and a unique EcoRI restriction in exon 2. The mutation changes 3 bp in the coding sequence of exon 2 as follows (numbering based on EP1 cDNA as reported in ref. 28): C795T causes in-frame stop codon R242X (CGA to TGA); C798G together with G799A introduces a new signature EcoRI site, allowing screening for the mutant gene by Southern analysis of EcoRI digests. The stop mutation halts translation at the beginning of the third

cytoplasmic loop of the EP1 receptor, resulting in a nonfunctional receptor. The normal sequence within the 5,067 bp of HindIII-XbaI fragment was replaced with mutant fragment, reconstituting EP1 with a stop at codon 242. The 5,067-kb mutant EP1 fragment was then subcloned into the plasmid pKOScrambler NTKV (Lexigen Inc.) that contains *neo* and TK selection cassettes.

Targeting the murine EP1 gene was accomplished by 2 steps using the hit-and-run strategy (25, 52). First, EP1 gene targeting vector was linearized by BstEII at a unique site between exons 1 and 2, prior to electroporation of TL-1 ES cells. The linearized mutant gene inserts along with the *neo* and TK gene were introduced into ES cells, allowing homologous recombination via a single crossover event that results in a direct repeat tandem duplication of the EP1 gene. Cells were grown for 5 days, insertion events were selected by G418 resistance, and resistant clones were isolated and confirmed by Southern blot using 3 DNA probes (probes A, B, and C) shown in Supplemental Figure 1. The detection of a 5.7-kb EcoRI fragment hybridizing probe A indicates targeting of the vector to the EP1 locus, while the wild-type locus, lacking the mutant EcoRI site in exon 2, yielded a 10-kb fragment (Figure 2). Screening EcoRI digests with probe C, composed of genomic sequence flanking the 3′ end of the EP1 gene, yielded an 11.5-kb fragment for events with the wild-type allele in the 3′ duplicate, documenting the insertion of an EcoRI site between *neo* and TK in the inserted vector (Supplemental Figure 1). The presence of the mutation in the 3′ duplicate resulted in a 4.3-kb fragment. In contrast, nontargeted EP1 loci yielded a 10-kb EcoRI fragment with all 3 probes. Second, because the direct repeat of the EP1 gene is unstable, spontaneous deletion of 1 allele arising via single, reciprocal intrachromosomal recombination occurred between the direct repeats, leading to deletion of the selectable cassettes, the plasmid backbone, and 1 repeat of the targeted loci. Targeted ES cells bearing the mutant allele were injected into blastocysts and introduced into a foster mother according to standard procedure carried out at Vanderbilt Transgenic Core.

Analysis of wild-type and targeted EP1 alleles. Both Southern blot– and PCR-based strategies were used for genotyping wild-type and EP1 mutant alleles. For Southern blot, mouse tail DNA digested with EcoRI was probed with a genomic DNA fragment (probe B; Supplemental Figure 1) using a standard protocol. For PCR analysis, a pair of primers was used to amplify a 1,066-bp genomic DNA fragment sparing the mutant site using the Advantage-GC Genomic PCR kit (BD Biosciences — Clontech). The sequences of the primers were as follows: sense, 5′-ACCAGCGCTGCCTATCTTCTCCAT-3′; antisense, 5′-GTCAACAAGCTGGGAACGAAAAAGGCTATGAA-3′. PCR reactions were carried out at 94°C for 30 seconds and 68°C for 3 minutes for 35 cycles. PCR products were then cut with EcoRI and separated on 1% agarose gel.

RNA expression analysis. Kidneys were harvested from $EP1^{+/+}$ and $EP1^{-/-}$ mice. Total RNA was extracted using TRIzol Reagent (Invitrogen), treated with RNAse-free DNAse I (Promega), and reverse-transcribed to single-stranded cDNA using Molony murine leukemia virus reverse transcriptase and 2.5 μM of random hexamers according to the manufacturer's protocol (GeneAmp RNA PCR kit; PerkinElmer Cetus). The synthesized cDNA was then used to amplify a portion of EP1 cDNA sparing the mutation site. The upstream sense primer was 5′-CACCTGGTGTTTTATTAGCCT-3′, and the downstream antisense primer was 5′-TTAGCTTCTTGGGCACATTCAG-3′. PCR reactions were carried out at 94°C for 30 seconds and 60°C for 60 seconds for 35 cycles in a PerkinElmer Cetus 2400 thermal cycler using the Advantage-GC cDNA PCR kit (BD Biosciences — Clontech). The predicted 780-bp fragment was sequenced and subjected to EcoRI digestion (Supplemental Figure 1B).

RT-PCR analysis of vascular expression of the EP1 mRNA. Total RNA was extracted from aortas and mesenteric arteries of $EP1^{+/+}$ mice and reverse-transcribed into cDNAs. The following set of primers specific for EP1 cDNA was used to examine EP1 mRNA expression: sense, 5′-TAACGATGGTCACGCGATGG-3′; antisense, 5′-ATGCAGTAGTGGGCTTAGGG-3′. The PCR conditions were the same as described in *RNA expression analysis*.

Expression of PKN in $EP1^{-/-}$ animals. Brain and kidney lysates (500 μg) prepared from $EP1^{-/-}$ mice and $EP1^{+/+}$ controls were resuspended in RIPA buffer containing proteases inhibitors and subjected to immunoprecipitation adding 2 μg of PKN C-19 goat polyclonal antibody (Santa Cruz Biotechnology Inc.). Samples were incubated overnight at 4°C on a rocking platform. Hydrated protein G CL4B (20 μl) was added to each sample and incubated for 1 hour at 4°C. Immunocomplexes were pelleted by a brief centrifugation at 13,000 *g*, and the supernatant was removed. The pellet was washed 3 times with RIPA buffer containing protease inhibitors, resuspended in a volume of Laemmli buffer, and boiled for 10 minutes. Solubilized immunocomplexes were resolved by 4%–20% gradient SDS-PAGE and transferred on PVDF membrane. Western blot analysis was performed using PKN C-19 goat polyclonal antibody (1:200 dilution) followed by a rabbit anti-goat horseradish peroxidase–conjugated secondary antibody (1:2,000 dilution).

Blood pressure measurement using tail-cuff and carotid catheterization in mice. Male congenic 129S6/SvEvTac or C57BL/6 mice aged 12–16 weeks and with 20–25 g body weight were used. Following a 2-week training period, basal blood pressure was measured in conscious $EP1^{+/+}$ and $EP1^{-/-}$ mice using the tail-cuff method as previously reported (29). These mice were then provided with normal-sodium diet for 2 days (0.25% w/w), followed by 4 days of low-salt diet (0.025%) and 4 days of high-salt diet (8% w/w). Urine was collected over 24-hour periods by housing mice in metabolic cages.

For infusion study, mice were anesthetized with 80 mg/kg ketamine (Fort Dodge Laboratories) and 8 mg/kg inactin (BYK) by i.p. administration. Mice were placed on a temperature-controlled pad. After tracheostomy, PE-10 tubing was inserted into the right carotid artery, a jugular vein catheter was placed for infusion, and a urinary bladder catheter was inserted for urine collection. Blood pressure was measured with a Cobe CDX II transducer connected to a blood pressure analyzer (BPA 400; Micromed) as previously reported (13, 29). The readings of blood pressure and heart rate were equilibrated for 30–60 minutes until stable values were obtained. The test agents (PGE_2, sulprostone, SC51322, 17-phenyltrinor PGE_2, and PGE_1-OH dissolved in absolute ethanol) were mixed with 25 μl of saline and injected as a bolus via the jugular vein. To examine the hypertensive response to Ang II in $EP1^{+/+}$ and $EP1^{-/-}$ mice, Ang II (Sigma-Aldrich) was dissolved in normal saline. Mice were continuously infused via carotid vein with Ang II at a rate of 75 pmol/kg/min for 30–45 minutes. Blood pressure, including systolic and diastolic pressure and MAP, and heart rates were recorded continuously on a thermal printer or computerized data record (13, 29).

Telemetric recording of blood pressure in SHRs. Male SHRs ($n = 5$) weighing approximately 250 g were used. Animals were anesthetized with phenobarbital (50 mg/kg i.p.), a midline abdominal incision was made, the intestines were displaced cranially, and the lower abdominal aorta was exposed. Vasospasm was reduced by the application of lidocaine 2% along the aorta. A small puncture was made in the aorta proximal to the femoral bifurcation, and the catheter of the transmitter was inserted and sealed in place with tissue adhesive (Vetbond; 3M Animal Care Products) and a cellulose patch (53). All procedures were performed aseptically. Following implantation, rats were returned to their home cages for monitoring and allowed to recover for 3 days prior to data collection. Continuous ambulatory systolic and diastolic blood pressure recordings were made via a radiofrequency receiver in conscious, unrestrained animals at a sampling rate of 64 Hz for 10 seconds, performed every 3 minutes for 1 hour (20 measurements), using the TA11PA-C20 pressure transmitter (Data Sciences International). Following surgery, the telemetry failed in 1 rat, which died; in another rat, the MAP was less than 110 mmHg, and so it was excluded from further experimentation. The remaining 3 animals were housed individually, and baseline heart

rate and MAP were determined for 6 days followed by a 3-day baseline blood pressure determination prior to treatment with the EP1 receptor antagonist for 3 days. MAP was monitored for 3 days during daily oral treatment with SC51322 (10 mg/kg) and for 2 days after discontinuation of treatment.

Establishment of Ang II–dependent hypertension. Ang II–dependent hypertension was induced in $EP1^{+/+}$ and $EP1^{-/-}$ mice (n = 5 per group) as previously reported (49). Briefly, Ang II (1,000 ng/kg/min; Sigma-Aldrich) dissolved in sterile saline or sterile saline alone for control animals was infused using an osmotic minipump (Alzet model 2004; Alza Corp.) that was inserted subcutaneously during an isoflurane anesthesia (3%). After 1 week of full recovery from the surgery, systolic blood pressure was recorded once a week for 1 month via computerized tail-cuff method. At the end of study, mice were anesthetized and catheters were inserted in carotid arteries and jugular veins. After 10-minute equilibration, MAP and heart rate were determined using a blood pressure analyzer (BPA 400; Micromed) as described above.

Renal microvascular responses. The perfused juxtamedullary nephron preparation was used to assess renal microvascular reactivity as described previously (54). Male C57BL/6 mice weighing 20–25 g were used. Mice were anesthetized with thiobutabarbital (inactin; 100 mg/kg i.p.). The kidney was removed and immediately isolated and perfused in vitro with a physiological salt solution and mixture of L–amino acids (54). The juxtamedullary vasculature was isolated for study, and an afferent arteriole was monitored continuously by videomicroscopy. After control diameter measurements, angiotensin (0.1–100 nM) or 17-phenyltrinor PGE_2 (1 μM) was delivered by superfusion, and the afferent arteriolar diameter response was determined. In a separate set of experiments, the response to angiotensin was determined in the presence of the EP1 antagonist SC51322 (1 μM).

Mesenteric arterial vascular tension. Mesenteric arteries (outer diameter, ~0.4 mm) of male C57BL/6 mice were dissected and cut into rings 5 mm in length in ice-cold modified Krebs-Ringer bicarbonate buffer (118.3 mM NaCl; 4.7 mM KCl; 2.5 mM $CaCl_2$; 1.2 mM $MgSO_4$; 1.2 mM KH_2PO_4; 25.0 mM $NaHCO_3$; and 11.1 mM glucose). Rings of mesenteric arteries were suspended in organ chambers filled with 15 ml of the modified Krebs-Ringer bicarbonate solution maintained at 37 ± 0.5°C and aerated with 95% O_2 and 5% CO_2 (pH 7.4). Two stirrups passed through the lumen suspended each ring. One stirrup was anchored to the bottom of the organ chamber and the other connected to a strain gauge, and the isometric force was measured with a ML785 PowerLab/8sp recording and Analysis System (ADInstruments) (55).

At the beginning of the experiment, each vessel ring was stretched to its optimal resting tension by step-wise stretching until the active contraction of the vessel ring to 100 mM KCl reached a plateau. The optimal resting tension of mouse mesenteric arteries was approximately 0.6 g. After the vessels were brought to their optimal resting tensions, 1 hour of equilibration was allowed. Concentration-response curves to Ang II were constructed in a cumulative fashion in vessels. In some experiments, SC51322, an EP1 receptor blocker, was administered to vessels at least 20 minutes prior to testing its effect contraction of the vessels evoked by Ang II.

Urine sodium and potassium measurement. Urine volumes were measured during perfusion study, and urinary sodium and potassium concentrations were analyzed using an IL943 Flame Photometer (Instrumentation Laboratory).

Construction of expression vectors with HA-tagged wild-type or mutant EP1 cDNA. RT-PCR was used to amplify a full-length mouse EP1 cDNA from kidney cDNA using the primers 5′-ATGAGCCCCTGCGGGCTTAACCTG-3′ and 5′-AGCTTCTGGGCACATTCAGAGGTG-3′. The PCR fragment was then subcloned into a pcDNA3 expression vector (Invitrogen) and sequenced. To facilitate in vitro detection of EP1 protein, a 45-bp human HA nucleotide fragment was inserted in-frame into upstream of mouse EP1 gene. The mouse EP1 mutant was generated by introducing a stop codon in the coding region of the EP1 receptor and creating a unique EcoRI restriction site using PCR-based mutagenesis. The mutation changes 3 bp in the coding sequence of exon 2 as follows (numbering based on EP1 cDNA as reported in ref. 28): C795T causes in-frame stop codon R242X (CGA to TGA); C798G together with G799A introduces a new signature EcoRI site, allowing screening for the mutant gene by EcoRI digests.

Measurement of $[Ca^{2+}]_i$ concentration. To confirm that the mutant EP1 protein lacks biological function, wild-type and mutant EP1 cDNAs were stably transfected into HEK293 cells. We estimated $[Ca^{2+}]_i$ from the emission intensity ratio using rapidly alternating 340/380 excitation on a PTI Deltascan spectrofluorometer coupled to a Nikon Diaphot and computer-based data acquisition system as previously reported (56).

Statistics. In all experiments, data were evaluated for significance by 2-tailed Student's t test, repeated-measures 2-way ANOVA, or 1-way ANOVA when appropriate, using Prism GraphPad 4.0 software. A P value less than 0.05 was considered statistically significant.

Acknowledgments

This work was supported by National Institute of Diabetes and Digestive and Kidney Disease grant DK-37097 (to M.D. Breyer). Funds were also provided by the Natural Science Foundation of China (30271521/30530340, to Y. Guan), the Ministry of Science and Technology (2006CB503906, to Y. Guan), National Institute of Diabetes and Digestive and Kidney Diseases grants DK65074 (to Y. Guan) and DK38226 (to J. Imig), and an American Heart Association Established Investigator Grant (to J. Imig). We also thank the staff of the Mouse Metabolic Phenotyping Center of Vanderbilt University School of Medicine, sponsored by NIH grant DK59637.

Received for publication July 24, 2006, and accepted in revised form May 29, 2007.

Address correspondence to: Matthew D. Breyer, Division of Nephrology, S-3223 Medical Center North, Vanderbilt University Medical Center, Nashville, Tennessee 37232-2372, USA. Phone: (615) 343-3764; Fax: (615) 343-4704; E-mail: breyerma@lilly.com. Or to: Youfei Guan, Department of Physiology and Pathophysiology, Peking University Health Science Center, 38 Xueyuan Road, Haidian District, Beijing 100083, People's Republic of China. Phone: 86-10-8280-1447; Fax: 86-10-8280-1447; E-mail: youfeiguan@bjmu.edu.cn.

1. Kobayashi, T., and Narumiya, S. 2002. Function of prostanoid receptors: studies on knockout mice. *Prostaglandins Other Lipid Mediat.* **68–69**:557–573.
2. Breyer, M.D., and Breyer, R.M. 2000. Prostaglandin E receptors and the kidney. *Am. J. Physiol. Renal Physiol.* **279**:F12–F23.
3. Cheng, H.F., and Harris, R.C. 2004. Cyclooxygenases, the kidney, and hypertension. *Hypertension.* **43**:525–530.
4. Izhar, M., Alausa, T., Folker, A., Hung, E., and Bakris, G.L. 2004. Effects of COX inhibition on blood pressure and kidney function in ACE inhibitor-treated blacks and hispanics. *Hypertension.* **43**:573–577.
5. Sowers, J.R., et al. 2005. The Effects of cyclooxygenase-2 inhibitors and nonsteroidal anti-inflammatory therapy on 24-hour blood pressure in patients with hypertension, osteoarthritis, and type 2 diabetes mellitus. *Arch. Intern. Med.* **165**:161–168.
6. Grosser, T., Fries, S., and FitzGerald, G.A. 2006. Biological basis for the cardiovascular consequences of COX-2 inhibition: therapeutic challenges and opportunities. *J. Clin. Invest.* **116**:4–15. doi:10.1172/JCI27291.
7. Gurwitz, J.H., et al. 1994. Initiation of antihypertensive treatment during nonsteroidal anti- inflammatory drug therapy. *JAMA.* **272**:781–786.
8. Qi, Z., et al. 2002. Opposite effects of cyclooxygenase-1 and -2 activity on the pressor response to angiotensin II. *J. Clin. Invest.* **110**:61–69. doi:10.1172/JCI200214752.
9. Breyer, M.D., and Breyer, R.M. 2001. G protein-coupled prostanoid receptors and the kidney. *Annu. Rev. Physiol.* **63**:579–605.
10. Qi, Z., Cai, H., Morrow, J.D., and Breyer, M.D. 2006. Differentiation of cyclooxygenase 1- and 2-derived

prostanoids in mouse kidney and aorta. *Hypertension.* **48**:323–328.
11. Narumiya, S., Sugimoto, Y., and Ushikubi, F. 1999. Prostanoid receptors: structures, properties, and functions. *Physiol. Rev.* **79**:1193–1226.
12. Tsuboi, K., Sugimoto, Y., and Ichikawa, A. 2002. Prostanoid receptor subtypes. *Prostaglandins Other Lipid Mediat.* **68–69**:535–556.
13. Kennedy, C.R., et al. 1999. Salt-sensitive hypertension and reduced fertility in mice lacking the prostaglandin EP2 receptor. *Nat. Med.* **5**:217–220.
14. Nadler, J., Zipser, R.D., Coleman, R., and Horton, R. 1983. Stimulation of renal prostaglandins by pressor hormones in man: comparison of prostaglandin E2 and prostacyclin (6 keto prostaglandin F1 alpha). *J. Clin. Endocrinol. Metab.* **56**:1260–1265.
15. Siragy, H.M., Senbonmatsu, T., Ichiki, T., Inagami, T., and Carey, R.M. 1999. Increased renal vasodilator prostanoids prevent hypertension in mice lacking the angiotensin subtype-2 receptor. *J. Clin. Invest.* **104**:181–188.
16. Takeuchi, K., et al. 1999. Prostaglandin E receptor subtypes involved in stimulation of gastroduodenal bicarbonate secretion in rats and mice. *J. Physiol. Pharmacol.* **50**:155–167.
17. Hallinan, E., Stapelfeld, A., Savage, M., and Reichman, M. 1994. 8-chlorodibenz[B,F][1, 4]oxazepine-10(11H)-carboxylic acid, 2-[3-2-(furanylmethyl)thio]-1-oxopropyl]hydrazide (SC51322): a potent PGE2 antagonist and analgesic. *Bioorg. Med. Chem. Lett.* **4**:509–514.
18. Hallinan, E.A., et al. 1993. N-substituted dibenzoxazepines as analgesic PGE2 antagonists. *J. Med. Chem.* **36**:3293–3299.
19. Stock, J.L., et al. 2001. The prostaglandin E2 EP1 receptor mediates pain perception and regulates blood pressure. *J. Clin. Invest.* **107**:325–331.
20. Batshake, B., and Sundelin, J. 1996. The mouse genes for the EP1 prostanoid receptor and the PKN protein kinase overlap. *Biochem. Biophys. Res. Commun.* **227**:70–76.
21. Mukai, H. 2003. The structure and function of PKN, a protein kinase having a catalytic domain homologous to that of PKC. *J. Biochem. (Tokyo).* **133**:17–27.
22. Pravenec, M., et al. 1999. Genetics of Cd36 and the clustering of multiple cardiovascular risk factors in spontaneous hypertension. *J. Clin. Invest.* **103**:1651–1657.
23. Hefferan, M.P., Carter, P., Haley, M., and Loomis, C.W. 2003. Spinal nerve injury activates prostaglandin synthesis in the spinal cord that contributes to early maintenance of tactile allodynia. *Pain.* **101**:139–147.
24. Ishibashi, R., et al. 1999. Roles of prostaglandin E receptors in mesangial cells under high-glucose conditions. *Kidney Int.* **56**:589–600.
25. Hasty, P., Ramirez-Solis, R., Krumlauf, R., and Bradley, A. 1991. Introduction of a subtle mutation into the Hox-2.6 locus in embryonic stem cells. *Proc. Natl. Acad. Sci. U. S. A.* **50**:243–246.
26. Guan, Y., et al. 1998. Prostaglandin E2 inhibits renal collecting duct Na+ absorption by activating the EP1 receptor. *J. Clin. Invest.* **102**:194–201.
27. Katoh, H., Watabe, A., Sugimoto, Y., Ichikawa, A., and Negishi, M. 1995. Characterization of the signal transduction of prostaglandin E receptor EP1 subtype in cDNA-transfected Chinese hamster ovary cells. *Biochim. Biophys. Acta.* **1244**:41–48.
28. Watabe, A., et al. 1993. Cloning and expression of cDNA for a mouse EP1 subtype of prostaglandin E receptor. *J. Biol. Chem.* **268**:20175–20178.
29. Zhang, Y., et al. 2000. Characterization of murine vasopressor and vasodepressor prostaglandin E(2) receptors. *Hypertension.* **35**:1129–1134.
30. Audoly, L.P., et al. 1999. Identification of specific EP receptors responsible for the hemodynamic effects of PGE2. *Am. J. Physiol.* **277**:H924–H930.
31. Zhang, Y., et al. 2000. Characterization of murine vasopressor and vasodepressor prostaglandin E2 receptors. *Hypertension.* **35**:1129–1134.
32. Durocher, Y., et al. 2000. A reporter gene assay for high-throughput screening of G-protein-coupled receptors stably or transiently expressed in HEK293 EBNA cells grown in suspension culture. *Anal. Biochem.* **284**:316–326.
33. Qi, Z., et al. 2002. Opposite effects of cyclooxygenase-1 and -2 activity on the pressor response to angiotensin II. *J. Clin. Invest.* **110**:61–69. doi:10.1172/JCI200214752.
34. Chatziantoniou, C., and Arendshorst, W.J. 1992. Impaired ability of prostaglandins to buffer renal vasoconstriction in genetically hypertensive rats. *Am. J. Physiol.* **263**:F573–F580.
35. Sugimoto, Y., Narumiya, S., and Ichikawa, A. 2000. Distribution and function of prostanoid receptors: studies from knockout mice. *Prog. Lipid Res.* **39**:289–314.
36. Breyer, M.D., Davis, L., Jacobson, H.R., and Breyer, R.M. 1996. Differential localization of prostaglandin E receptor subtypes in human kidney. *Am. J. Physiol.* **270**:F912–F918.
37. Ahn, D., et al. 2004. Collecting duct–specific knockout of endothelin-1 causes hypertension and sodium retention. *J. Clin. Invest.* **114**:504–511. doi:10.1172/JCI200421064.
38. Hébert, R., Jacobson, H., and Breyer, M. 1990. PGE2 inhibits AVP induced water flow in cortical collecting ducts by protein kinase C activation. *Am. J. Physiol.* **259**:F318–F325.
39. Yang, T., et al. 1998. Regulation of cyclooxygenase expression in the kidney by dietary salt intake. *Am. J. Physiol.* **274**:F481–F489.
40. Batshake, B., Nilsson, C., and Sundelin, J. 1995. Molecular characterization of the mouse prostanoid EP1 receptor gene. *Eur. J. Biochem.* **231**:809–814.
41. Boie, Y., et al. 1997. Molecular cloning and characterization of the four rat prostaglandin E2 prostanoid receptor subtypes. *Eur. J. Pharmacol.* **340**:227–241.
42. Kiriyama, M., et al. 1997. Ligand binding specificities of the eight types and subtypes of the mouse prostanoid receptors expressed in Chinese hamster ovary cells. *Br. J. Pharmacol.* **122**:217–224.
43. Rao, R., et al. 2007. Prostaglandin E2-EP4 receptor promotes endothelial cell migration via ERK activation and angiogenesis in vivo. *J. Biol. Chem.* **282**:16959–16968.
44. Southall, M.D., and Vasko, M.R. 2001. Prostaglandin receptor subtypes, EP3C and EP4, mediate the prostaglandin E2-induced cAMP production and sensitization of sensory neurons. *J. Biol. Chem.* **276**:16083–16091.
45. Kubo, S., et al. 2004. E-prostanoid (EP)2/EP4 receptor-dependent maturation of human monocyte-derived dendritic cells and induction of helper T2 polarization. *J. Pharmacol. Exp. Ther.* **309**:1213–1220.
46. Ohnaka, K., Numaguchi, K., Yamakawa, T., and Inagami, T. 2000. Induction of cyclooxygenase-2 by angiotensin II in cultured rat vascular smooth muscle cells. *Hypertension.* **35**:68–75.
47. Purdy, K.E., and Arendshorst, W.J. 1999. Prostaglandins buffer ANG II-mediated increases in cytosolic calcium in preglomerular VSMC. *Am. J. Physiol.* **277**:F850–F858.
48. Satoh, H., and Satoh, S. 1984. Prostaglandin E2 and I2 production in isolated dog renal arteries in the absence or presence of vascular endothelial cells. *Biochem. Biophys. Res. Commun.* **118**:873–876.
49. Francois, H., Athirakul, K., Mao, L., Rockman, H., and Coffman, T.M. 2004. Role for thromboxane receptors in angiotensin-II-induced hypertension. *Hypertension.* **43**:364–369.
50. Crowley, S.D., et al. 2005. Distinct roles for the kidney and systemic tissues in blood pressure regulation by the renin-angiotensin system. *J. Clin. Invest.* **115**:1092–1099. doi:10.1172/JCI200523378.
51. Negus, P., Tannen, R.L., and Dunn, M.J. 1976. Indomethacin potentiates the vasoconstrictor actions of angiotensin II in normal man. *Prostaglandins.* **12**:175–180.
52. MacMillan, L.B., Hein, L., Smith, M.S., Piascik, M.T., and Limbird, L.E. 1996. Central hypotensive effects of the alpha2a-adrenergic receptor subtype. *Science.* **273**:801–803.
53. Schyvens, C.G., Mangos, G.J., Zhang, Y., McKenzie, K.U., and Whitworth, J.A. 2001. Telemetric monitoring of adrenocorticotrophin-induced hypertension in mice. *Clin. Exp. Pharmacol. Physiol.* **28**:758–760.
54. Imig, J.D., Breyer, M.D., and Breyer, R.M. 2002. Contribution of prostaglandin EP(2) receptors to renal microvascular reactivity in mice. *Am. J. Physiol. Renal Physiol.* **283**:F415–F422.
55. Wang, X., Tong, M., Chinta, S., Raj, J.U., and Gao, Y. 2006. Hypoxia-induced reactive oxygen species downregulate ETB receptor-mediated contraction of rat pulmonary arteries. *Am. J. Physiol. Lung Cell Mol. Physiol.* **290**:L570–L578.
56. Breyer, M.D. 1991. Feedback inhibition of cyclic adenosine monophosphate-stimulated Na+ transport in the rabbit cortical collecting duct via Na(+)-dependent basolateral Ca++ entry. *J. Clin. Invest.* **88**:1502–1510.